Neuron 43, 219–232, January 19, 2004 ©2004 Elsevier Inc. DOI 10.1016/j.neuron.2004.06.029

Signaling Mechanisms Underlying Slit2-Induced Collapse of *Xenopus* Retinal Growth Cones

Michael Piper,[1] Richard Anderson,[1,2] Asha Dwivedy,[1] Christine Weinl,[1] Francis van Horck,[1] Kin Mei Leung,[1] Emily Cogill,[1] and Christine Holt[1,*]
[1] Department of Physiology, Development and Neuroscience
University of Cambridge
Downing Street
Cambridge
United Kingdom

Summary

Slits mediate multiple axon guidance decisions, but the mechanisms underlying the responses of growth cones to these cues remain poorly defined. We show here that collapse induced by Slit2-conditioned medium (Slit2-CM) in *Xenopus* retinal growth cones requires local protein synthesis (PS) and endocytosis. Slit2-CM elicits rapid activation of translation regulators and MAP kinases in growth cones, and inhibition of MAPKs or disruption of heparan sulfate blocks Slit2-CM-induced PS and repulsion. Interestingly, Slit2-CM causes a fast PS-dependent decrease in cytoskeletal F-actin concomitant with a PS-dependent increase in the actin-depolymerizing protein cofilin. Our findings reveal an unexpected link between Slit2 and cofilin in growth cones and suggest that local translation of actin regulatory proteins contributes to repulsion.

Introduction

Developing retinal ganglion cell (RGC) axons navigate to targets in the brain along a stereotypical pathway. Environmental cues act as attractants or repellents, serving as molecular signposts to ensure the fidelity of navigation (Dickson, 2002). One such family of secreted repulsive cues are the Slits, whose role in axon guidance has been highly conserved during evolution. For instance, Slits have been implicated in the repulsion of commissural axons from both the ventral midline of *Drosophila* (Kidd et al., 1999) and the spinal cord floor-plate of mammals (Long et al., 2004). In vertebrate RGC axon guidance, Slit2 is a repellent for retinal neurites in vitro, and expression of Slit1 and -2 around the developing chiasm may restrict retinal axon growth to a narrow, Slit-free channel across the midline (Erskine et al., 2000; Niclou et al., 2000; Ringstedt et al., 2000). Supporting this, *Slit1/2* double mutant mice often exhibit defects in RGC axon guidance, including ectopic chiasm formation (Plump et al., 2002). Robo2, a Slit receptor, is expressed in RGCs (Niclou et al., 2000), and the zebrafish *astray* (a Robo2 homolog) mutant (Fricke et al., 2001; Hutson and Chien 2002) exhibits major pathfinding defects, with axons straying from the optic tract and invading inappropriate territories. Thus, Slits are potent regulators of axon navigation in the visual pathway.

Some recent progress has been made toward understanding the regulation and identification of downstream targets of the Slits. For example, Slit function can be regulated by heparan sulfate (HS) proteoglycans (Hu, 2001; Johnson et al., 2004; Lee et al., 2004b). The enormous range of molecular diversity able to be imparted on heparan sulfate side chains through differential sulfation and epimerization (Bulow and Hobert, 2004) may allow precise control of receptor-ligand binding. At the intracellular level, some downstream targets of Slit signaling have been identified, such as members of the Rho GTPase-activating protein family, that may act to regulate cytoskeletal behavior in response to this cue (Lundstrom et al., 2004; Wong et al., 2001). Genetic studies have also implicated a number of proteins downstream of Robo in the process of cytoskeletal rearrangement in *Drosophila*, including the tyrosine kinase Abelson and its substrate, the actin binding protein Enabled (Bashaw et al., 2000); the adaptor protein Dreadlocks; and the p21-activated serine-threonine kinase Pak (Fan et al., 2003); Capulet, an adenylyl cyclase-associated protein capable of binding actin (Wills et al., 2002); and Orbit/MAST, a microtubule plus-end tracking protein (Lee et al., 2004a). However, a number of questions remain uncharacterized with respect to the role of Slit2 in guiding RGC axons. First, it is unknown whether Slit2 plays a role in axon guidance later in the optic pathway, when the retinal axons are approaching their targets in the brain. Second, we are still a long way from understanding how the receptor/ligand interaction is regulated in the milieu of the optic pathway and how this interaction is linked to the cytoskeleton to elicit a chemotropic response. The purpose of this study was to address these issues, using the retinotectal projection of *Xenopus* as a model system.

We demonstrate that the response of retinal neurites to Slit2 (a homolog of *Xenopus* Slit) conditioned medium (Slit2-CM) is developmentally regulated, occurring only in late-stage RGC growth cones and that Slit is expressed at the dorsal midline and around the anterior and posterior margins of the optic tectum when retinal axons are entering this zone. Using various in vitro assays, we show that Slit2-CM triggers protein synthesis (PS) within isolated growth cones. Furthermore, using pharmacological inhibitors, we demonstrate that PS, but not proteasomal degradation, is an essential element of collapse induced by Slit2-CM and that HS and endocytosis are involved in chemotropic responses. We also identify some of the signaling events involved, showing that the mitogen-activated protein kinases (MAPKs) p38 and p42/p44 are rapidly activated following Slit2-CM application, as is the translational regulator Mnk-1 and the translation initiation regulators eIF4E and eIF4EBP-1. Finally, we identify cofilin, an actin-depolymerizing protein, as a potential candidate to be translated in response to this cue. These data suggest that

*Correspondence: ceh@mole.bio.cam.ac.uk
[2] Present address: Department of Anatomy & Cell Biology, University of Melbourne, Australia
Dedicated to the memory of Emily Cogill, deceased on July 7, 2004.

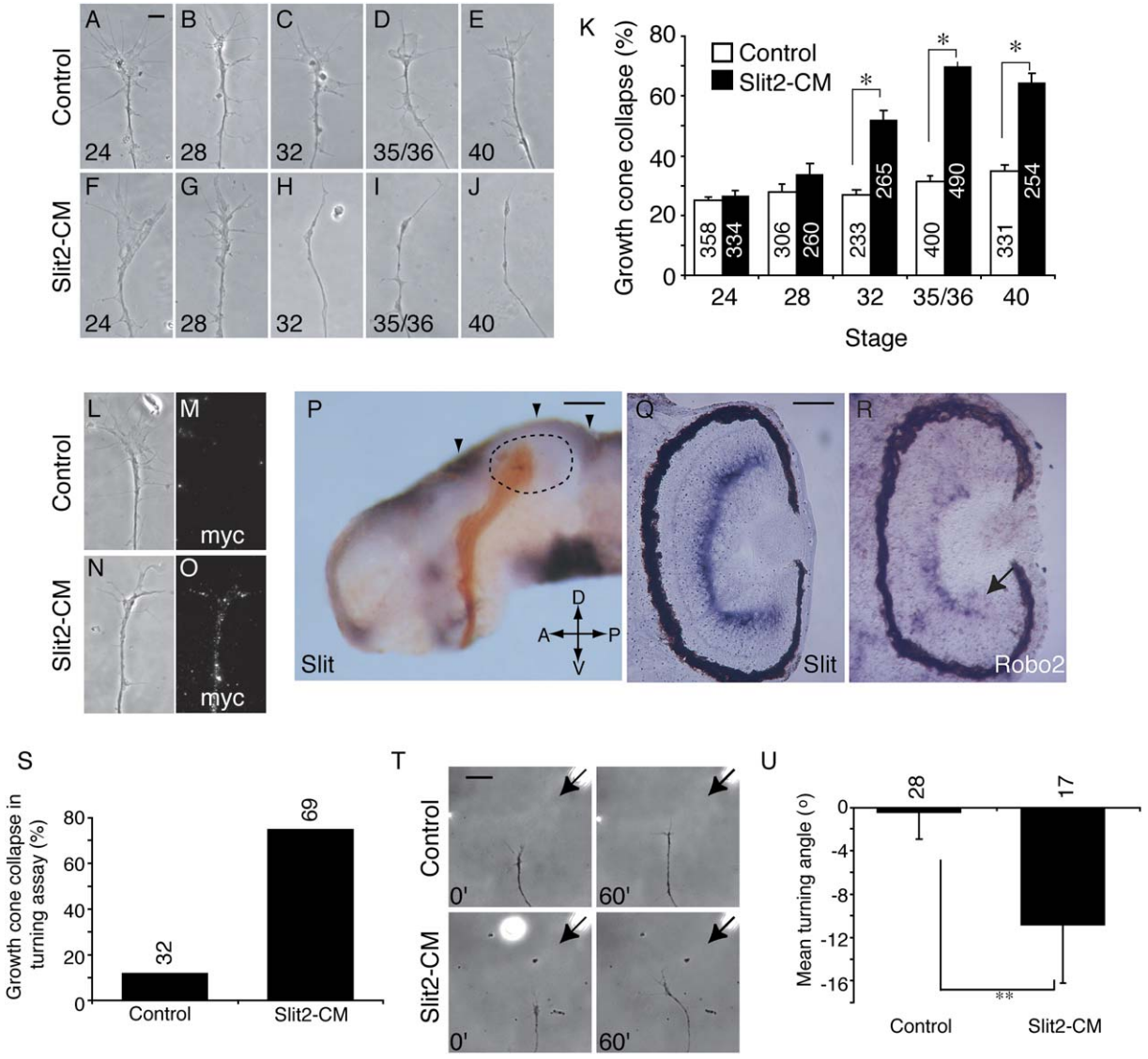

Figure 1. Slit2-CM Causes Turning and Developmentally Regulated Collapse

Retinal explants from stage 24 (A and F), 28 (B and G), 32 (C and H), 35/36 (D and I), and 40 (E and J) embryos were cultured for 24 hr prior to addition of Slit2-CM or control for 10 min. Slit2-CM caused growth cone collapse in those explants taken from embryos at stage 32 or later (K). After 2 min, Slit2 bound to the surface of cultured stage 35/36 growth cones was detected with an antibody against the *myc* epitope (L–O). An isolated brain at stage 40, with retinal axons (brown) entering the tectum (delineated with dotted lines), exhibits Slit mRNA (purple) expression at the dorsal midline and at the anterior and posterior margins of the tectum (arrowheads, [P]). Expression of Slit is also seen in the inner plexiform layer of the eye at stage 40 (Q). Developing RGCs at the periphery of the retina express Robo2 at stage 40 (arrow, [R]), and transcript is also seen in the inner nuclear layer. In turning assays, Slit2-CM caused a high level of collapse compared to the control (S). In those growth cones that did not collapse (T), Slit2-CM caused repulsive turning (U). Numbers inside bars denote growth cones tested. *$p < 0.03$, Mann-Whitney U test; **$p < 0.05$, t test. Scale bars: 10 μm (A–J), (L–O), 200 μm (P), 75 μm (Q and R), 20 μm (T).

Slit may help to corral axons into the tectum and define a mechanism for eliciting cytoskeletal changes in response to this ligand, whereby local synthesis of cofilin in the growth cone may mediate actin depolymerization and repulsion.

Results

Slit2-CM Causes Collapse and Repulsive Turning in Late-Stage RGC Growth Cones

As retinal growth cones age, they gain responsiveness to Sema3A and lose attraction to netrin-1 (Campbell et al., 2001; Shewan et al., 2002). To investigate whether Slit2 responsiveness is developmentally regulated, we used in vitro collapse assays to analyze its effects on growth cones of *Xenopus* retinal explants from a range of ages. Retinal explants from stages 24, 28, 32, 35/36, and 40 were cultured for 24 hr prior to addition of Slit2-CM (or control; Figures 1A–1J). Slit2-CM caused significant collapse compared to controls only in explants cultured from stage 32 or later (Figure 1K). Binding of the *myc*-tagged Slit2 to cultured stage 35/36 growth cones was detected immunohistochemically using an anti-*myc* antibody (Figures 1L–1O). The acquisition of a repulsive

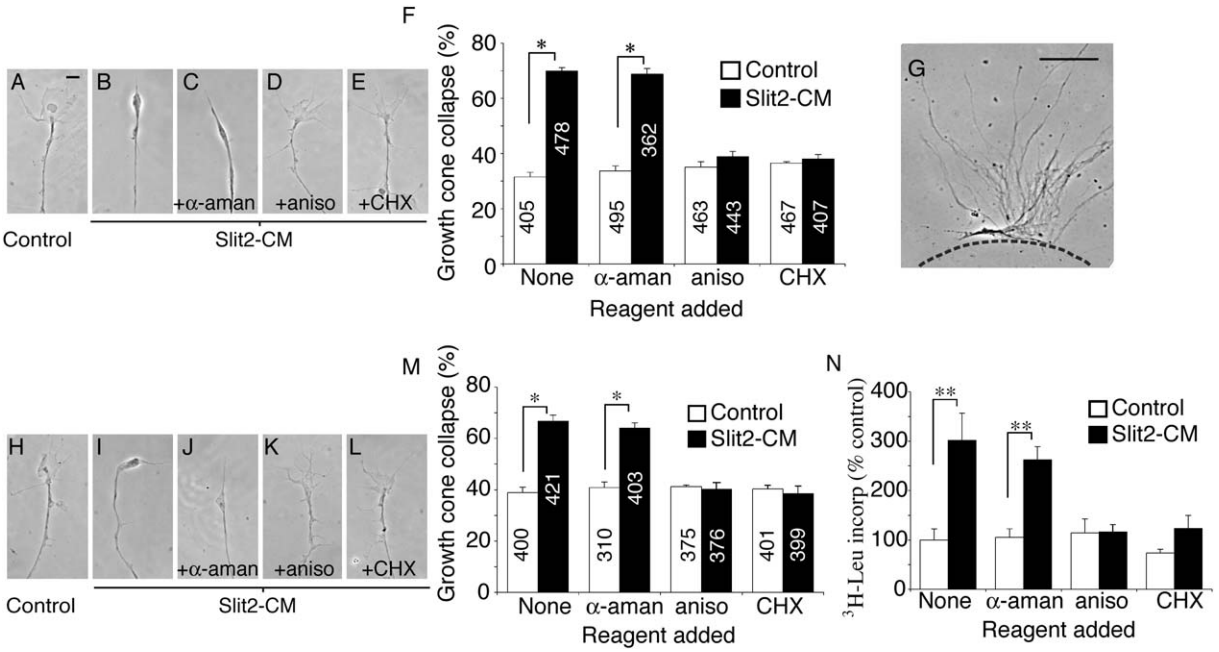

Figure 2. Collapse Is Blocked by Protein Synthesis Inhibitors

Slit2-CM triggers collapse of cultured stage 35/36 retinal growth cones (A and B). Collapse is not affected by the transcriptional inhibitor α-aman, but is blocked by the translational inhibitors aniso and CHX (C–F). To investigate whether this was a local effect, explants were removed prior to the assay being performed (G). Cue-induced collapse was still blocked by translational inhibitors (H–M). Slit2-CM increased the uptake of TCA-precipitated ^{3}H leucine in isolated growth cones in comparison to the control. This effect was inhibited by aniso and CHX, but not by α-aman (N). The counts observed in the aniso- and CHX-treated samples may reflect tRNA-bound ^{3}H leucine. Numbers inside bars denote growth cones tested. *$p < 0.03$, Mann-Whitney U test; **$p < 0.01$, Kruskal-Wallis test. Scale bars: 10 μm (A–E and H–L), 100 μm (G).

response in older growth cones suggests that responses to this ligand are developmentally regulated. Interestingly, the highest level of collapse (69.9% ± 1.25%) was seen in 24 hr cultures of stage 35/36 retinal explants; this corresponds to approximately stage 39–40 in vivo, when the RGC axons have begun to enter the optic tectum, and suggests that Slit mediates RGC axon-guidance decisions in the distal optic tract and tectum.

We next investigated Slit expression in stage 40 *Xenopus* embryonic brains. In situ hybridization revealed Slit expression along the dorsal midline and around the anterior and posterior margins of the optic tectum (Figure 1P). RGC axons avoid these regions, which is consistent with the collapse-inducing activity of Slit2-CM in vitro and is indicative of a role in confining RGC axons to the tectum. Slit expression was also detected in the diencephalon just anterior to the optic tract, in the cells surrounding the optic chiasm and in the inner plexiform layer of the eye (Figure 1Q). We also analyzed the expression of the Slit receptors, Robo1 and Robo2, at stage 40. We were unable to detect Robo1 expression in the eye, but observed Robo2 transcripts in peripherally positioned RGCs and in cells of the inner nuclear layer of the central retina (Figure 1R).

We then performed a second chemotropic assay, the growth cone turning assay, to confirm that Slit2 was indeed a repellent for RGC axons. Growth cones from 24 hr cultures of stage 35/36 retinal explants have previously been shown to be repelled by gradients of Sema3A and netrin-1 (Campbell et al., 2001; Shewan et al., 2002). Unlike these molecules, a gradient of Slit2-CM caused a high level of growth cone collapse (Figure 1S). However, in those growth cones that did not collapse, Slit2-CM induced repulsive turning in comparison to controls (Figures 1T and 1U). Using a less concentrated source of the cue mitigated collapse, but abolished the repulsive turning response (data not shown). These data support the idea that Slit2 acts to repel late-stage *Xenopus* RGC growth cones. We then sought to determine the molecular mechanisms underlying the Slit2-induced collapse of growth cones from 24 hr cultures of stage 35/36 retinal explants.

Local Protein Synthesis Is Required for Slit-Induced Collapse

The chemotropic responses of *Xenopus* retinal growth cones to netrin-1 and Sema3A are known to require local protein synthesis (PS) (Campbell and Holt, 2001). To investigate whether collapse in response to Slit2-CM was also reliant on PS, collapse assays were performed in the presence of the translation inhibitors anisomycin (aniso) and cycloheximide (CHX). Collapse induced by Slit2-CM was blocked by aniso and CHX, but not by the transcription inhibitor α-amanitin (α-aman; Figures 2A–2F). Although the necessary elements for protein synthesis, including mRNA, tRNA, and ribosomes, have been identified in axons (Alvarez et al., 2000; Piper and Holt, 2004), the PS necessary for collapse may take place in the cell body or in the axon/growth cone compartment. To differentiate between these possibilities, retinal neurites were severed and explants removed prior to performing the assay (Figure 2G). The response of isolated growth cones to Slit2-CM was again inhibited by aniso and CHX, but not by α-aman (Figures 2H–2M). To directly

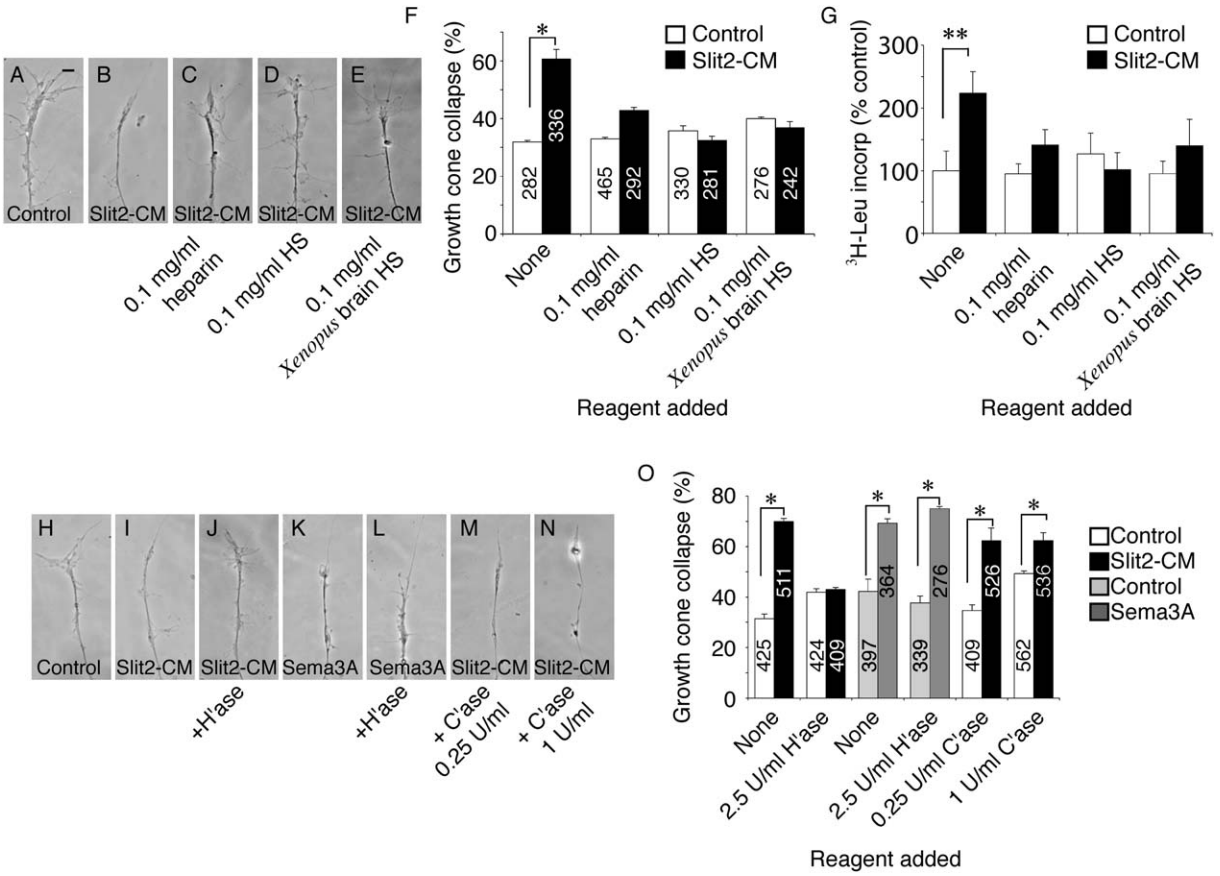

Figure 3. Heparan Sulfate Is Essential for Slit-Induced Protein Synthesis and Collapse

In cultured stage 35/36 retinal explants, Slit2-CM-induced collapse of growth cones is inhibited by the addition of heparin, bovine HS, or HS extracted from embryonic *Xenopus* brains (A–F). These HSs also inhibited cue-induced PS in isolated neurites (G). Removal of HS moieties via pretreatment with heparinase I (H'ase) resulted in a failure of growth cones to collapse in response to Slit2-CM (H–J and O). Sema3A-induced collapse was unaffected by H'ase treatment (K, L, and O). Pretreatment of explants with chondroitinase ABC (C'ase) did not affect collapse of growth cones caused by Slit2-CM (M–O). Numbers inside bars denote growth cones tested. *$p < 0.03$, Mann-Whitney U test; **$p < 0.05$, Kruskal-Wallis test. Scale bar: 10 μm.

assay for protein synthesis within isolated growth cones, ^{3}H-leucine was added concurrently with Slit2-CM. After 10 min, trichloroacetic acid (TCA) was used to precipitate proteins in situ on the coverslips, and isotope uptake was measured with a scintillation counter. Slit2-CM elicited a significant increase in ^{3}H-leucine uptake in comparison to the control. This effect was abolished when aniso or CHX, but not α-aman, was present (Figure 2N). These data support the notion that Slit2 triggers local PS within the growth cone and that this is required for subsequent chemotropic responses.

Slit-Induced Collapse and Protein Synthesis Depend on Heparan Sulfate

Although Robos are the cognate Slit receptors, other molecules may also modulate the receptor/ligand interaction. In this respect, heparan sulfate proteoglycans (HSPGs) are especially interesting. The *Drosophila* HSPG syndecan forms complexes with Slit and Robo and interacts genetically with both of these molecules (Johnson et al., 2004; Steigemann et al., 2004). Furthermore, vertebrate Slit2 is able to bind the HSPG glypican-1 (Ronca et al., 2001), and enzymatic disruption of HS chains abrogates the repulsive activity of Slit2 in vitro (Hu, 2001). Previous studies have shown that the addition of exogenous HS to exposed *Xenopus* brains in vivo disrupts RGC axon entry into the tectum (Walz et al., 1997). We hypothesized that if HS chains were involved in modulating Slit/Robo binding, addition of exogenous HS may competitively inhibit this event by saturating relevant sites of interaction.

To address this, we added HS to cultured retinal explants immediately prior to Slit2-CM addition in the collapse assay. When heparin, HS (bovine), or HS extracted from embryonic *Xenopus* brains was present in the medium, Slit2-CM did not elicit significant growth cone collapse (Figures 3A–3F). Similarly, addition of these HSs to isolated growth cones diminished ^{3}H-leucine uptake in Slit2-CM-treated samples to a level comparable to controls (Figure 3G). This suggests that HS may indeed regulate chemotropic responses to this guidance cue. However, these data do not rule out nonspecific blocking of ligand/receptor interactions.

To clarify this, we next treated retinal explants with heparinase I (H'ase) at a concentration known to effectively remove HS from retinal axons (Walz et al., 1997) before performing collapse assays. After H'ase treatment, growth cones exhibited only a basal level of collapse to

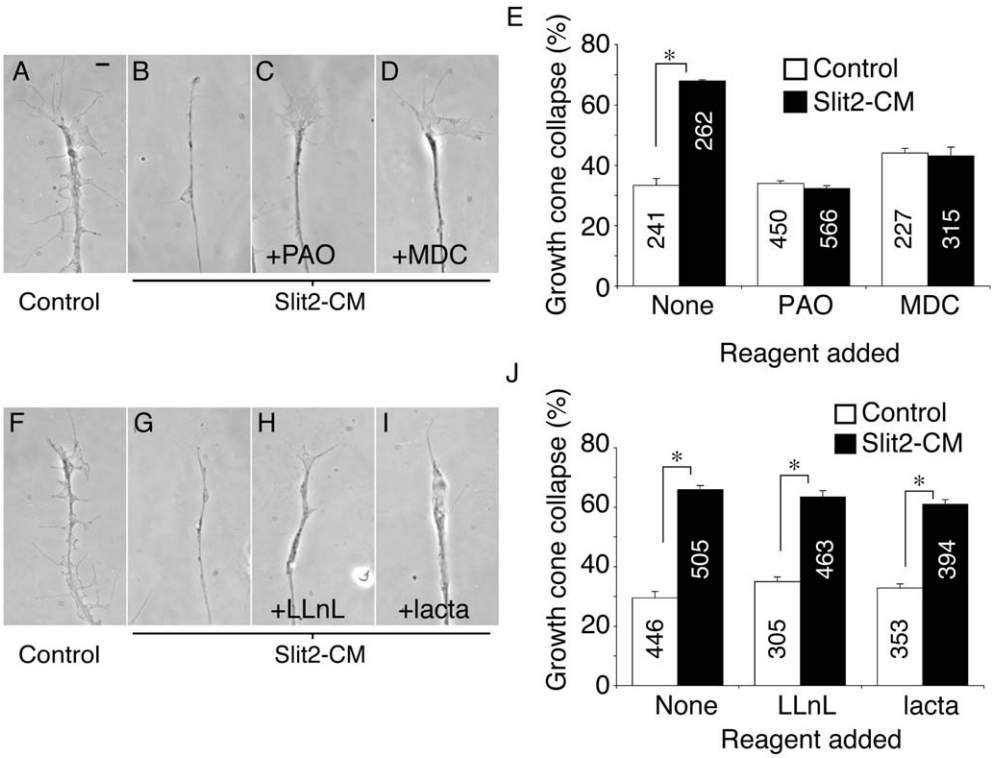

Figure 4. Endocytosis, but Not Degradation, Is Required for Slit-Induced Collapse

The collapse of retinal growth cones after application of Slit2-CM for 10 min (A and B) was reduced to background levels when the endocytosis inhibitors PAO (C) or MDC (D) were present during the assay (E). Conversely, the proteasomal inhibitors LLnL and lacta did not block growth cone collapse induced by this cue (F–J). Numbers inside bars denote growth cones tested. *$p < 0.03$, Mann-Whitney U test. Scale bar: 10 μm.

Slit2-CM, indicative of a loss in sensitivity to this cue (Figures 3H–3J and 3O). This was specific, as collapse induced by another repulsive cue, Sema3A, was unaffected by H'ase treatment (Figures 3K, 3L, and 3O). Finally, treatment of cultures with chondroitinase ABC (C'ase), to remove chondroitin sulfate (CS), did not alter the collapse response of growth cones to Slit2-CM (Figures 3M–3O), demonstrating a requirement for HS, but not CS. These data are consistent with a role for HSPGs in the modulation of growth cone responses to Slit2 and provide evidence that cue-induced translation leading to chemotropic collapse may be regulated at the level of the receptor/ligand interaction by HS side chains.

Differential Requirement for Endocytosis and Protein Degradation in Collapse

Endocytosis may play an integral role in chemotropic signaling. For example, Sema3A enhances endocytosis in growth cones in vitro (Castellani et al., 2004; Fournier et al., 2000), the endocytic internalization of EphB/ephrinB complexes may be important for axon withdrawal during collapse (Mann et al., 2003; Zimmer et al., 2003), and we have recently shown that endocytosis is an essential component of cue-induced growth cone desensitization (Piper et al., 2005). We investigated whether endocytosis was needed for Slit2-elicited collapse by using the nonspecific endocytosis inhibitor phenylarsine oxide (PAO). Blocking endocytosis with PAO during the 10 min assay inhibited collapse in response to Slit2-CM (Figures 4A–4C and 4E). To determine which endocytic pathway may be involved, we next used monodansyl cadaverine (MDC), a specific inhibitor of clathrin-mediated endocytosis (Ray and Samanta, 1996). MDC also blocked collapse of retinal growth cones after Slit2-CM application (Figures 4D and 4E). Clathrin-mediated endocytosis may be an essential component of the chemotropic response of RGC growth cones to this cue. Proteasomal degradation has also been implicated in repulsion induced by netrin-1 and lysophosphatydic acid (LPA) (Campbell and Holt, 2001). We used the proteasomal inhibitors LLnL and lactacystin (lacta) to investigate whether the response of retinal growth cones to Slit2 required protein breakdown. Neither LLnL nor lacta (Figures 4F–4J) decreased Slit2-CM-induced collapse, implying that, like Sema3A (Campbell and Holt, 2001), Slit2 does not rely on proteasomal degradation to promote growth cone collapse.

mTOR and MAPKs Are Involved in Slit-Induced Collapse and Protein Synthesis

To further characterize relevant downstream pathways, we used different kinase inhibitors in both the collapse and ^{3}H-leucine incorporation assays. In contrast to a previous report (Wong et al., 2004), inhibition of PI-3 kinase with wortmannin (Wort) had no effect on Slit2-CM-induced collapse or PS (Figures 5A–5F), implying that this kinase is not used in this developmental context. Another kinase involved in chemotropic responses of RGC growth cones is mammalian target of rapamycin (mTOR) (Campbell and Holt, 2001). mTOR is a key mediator of cap-dependent translation; blockade of mTOR with rapamycin (Rapa) inhibited both growth cone

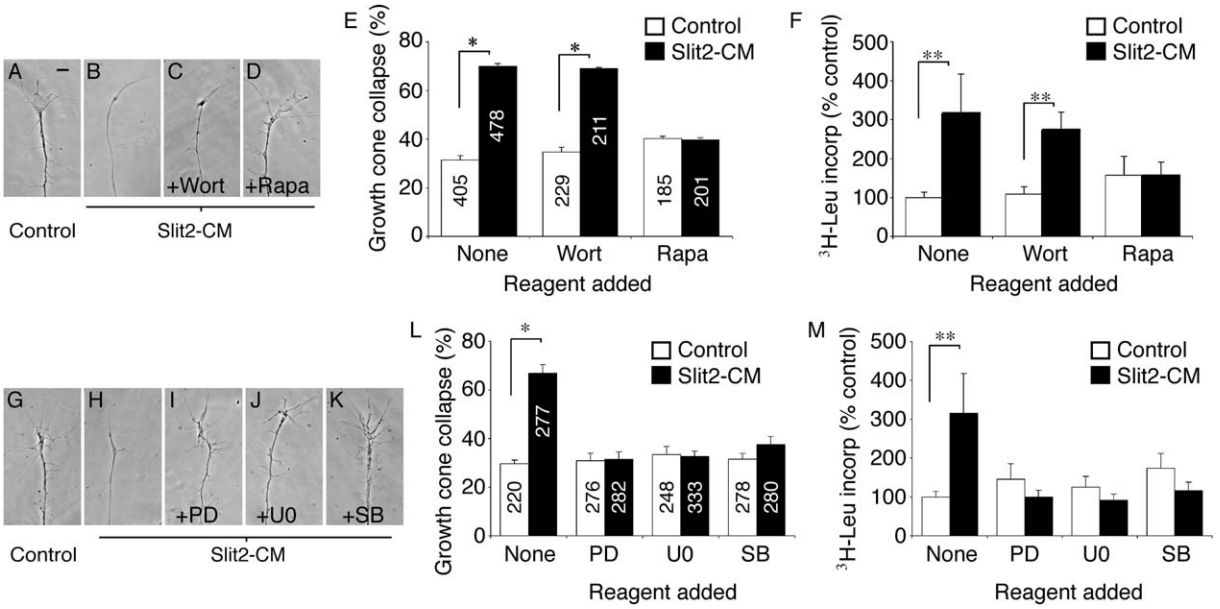

Figure 5. Inhibition of Signaling Pathways Can Block Collapse and Protein Synthesis

Specific kinase inhibitors were used to identify signaling components involved in eliciting collapse and PS in response to Slit2-CM. Wortmannin (Wort), an inhibitor of PI-3 kinase, had no effect on collapse (A–C and E) or PS (F), unlike rapamycin (Rapa), which did inhibit collapse (D and E) and PS (F). Similarly, inhibition of the MAPKs MEK1 and MEK2 with PD98059 (PD) or U0126 (U0), and the MAPK p38 with SB203580 (SB), resulted in an abrogation of collapse (G–L) and PS (M) following application of Slit2-CM. Numbers inside bars denote growth cones tested. *$p < 0.03$, Mann-Whitney U test; **$p < 0.05$, Kruskal-Wallis test. Scale bar: 10 μm.

collapse and PS in response to Slit2-CM (Figures 5A–5F). Finally, we blocked MAPK activity with specific inhibitors. Blocking MEK1 and MEK2 function with either PD98059 (PD) or U0126 (U0) abolished Slit2-CM-induced collapse and PS, as did blocking p38 activity with SB203580 (SB; Figures 5G–5M).

Slit Causes Rapid Activation of MAPKs and Translational Regulators

Because our results implicated MEK1/MEK2 and p38 in Slit signaling, we next sought to monitor the activation of selected MAPK proteins. To do this, we bath-applied Slit2-CM to retinal cultures for 5 min, then labeled active (phosphorylated) MAPK proteins with phospho-specific antibodies and used digital quantitation of immunofluorescence (see Experimental Procedures) to monitor relative changes in signal intensity. Five minutes was selected because a collapse assay time course (data not shown) showed that 40.3% ± 1.66% of growth cones collapsed 5 min after Slit2-CM addition. Thus, we reasoned that this time point would be optimal for assessing the signaling events leading to collapse, prior to the occurrence of overt collapse. Using a phosphospecific p38 antibody (p38-P), we found that Slit2-CM stimulated an ~80% increase in signal intensity compared to controls (Figures 6A–6C). The MAPK p42/p44 can be directly phosphorylated by MEK1/MEK2 (Raught and Gingras, 1999). After Slit2-CM application, we also saw a 2-fold rise in phospho-p42/p44 fluorescent intensity (p42/p44-P; Figures 6D–6F). Slit2-CM did not have a significant effect on the fluorescent intensity of either p38 (p38-Total) or p42/p44 (p42/p44-Total; Figures 6A–6D).

Initiation of translation requires the assembly of multiple proteins into a translation complex, including the translation initiation factor 4E (eIF4E). When outside the complex, eIF4E is unphosphorylated and bound by a repressor, the binding protein eIF4EBP-1. Phosphorylation of the repressor allows release of eIF4E, which is then phosphorylated itself prior to joining the translation complex. Thus, phosphorylation of eIF4E and eIF4EBP-1 can be correlated to initiation of mRNA translation (Raught and Gingras, 1999). Both p38 and p42/p44 can phosphorylate and activate the kinase Mnk-1. Mnk-1-P in turn can phosphorylate and activate eIF4E (Raught and Gingras, 1999). After 5 min, Slit2-CM caused an ~90% increase in the signal intensity of Mnk-1-P (Figures 6G–6I). Our earlier data suggested that Slit2-CM does not act via PI-3 kinase (Figure 5E). Using a phosphospecific PI-3 kinase antibody, we found that the signal intensity of PI3 kinase-P did not significantly change after 5 min Slit2-CM stimulation. Furthermore, these growth cones were costained with Mnk-1-P, whose relative intensity levels rose significantly in response to Slit2-CM (data not shown), showing the rise in Mnk-1 phosphorylation to be specific. Finally, Slit2-CM caused a significant increase in fluorescent intensity of the active, phosphorylated form of eIF4E (eIF4E-P) and the phosphorylated (i.e., inactive) form of its repressor (eIF4EBP-1-P), while the intensity of the total amounts of these proteins was unchanged (Figures 6J–6O). Although we stained for each kinase independently in these experiments, we also performed experiments in which stimulated growth cones were stained with eIF4EBP-1-Total and eIF4EBP-1-P antibodies concurrently. A significant rise in phosphorylated, but not total, eIF4EBP-1 fluorescent intensity was again observed (data not shown). Thus, Slit2-CM is able to activate two major MAPK pathways and to relieve the repression of

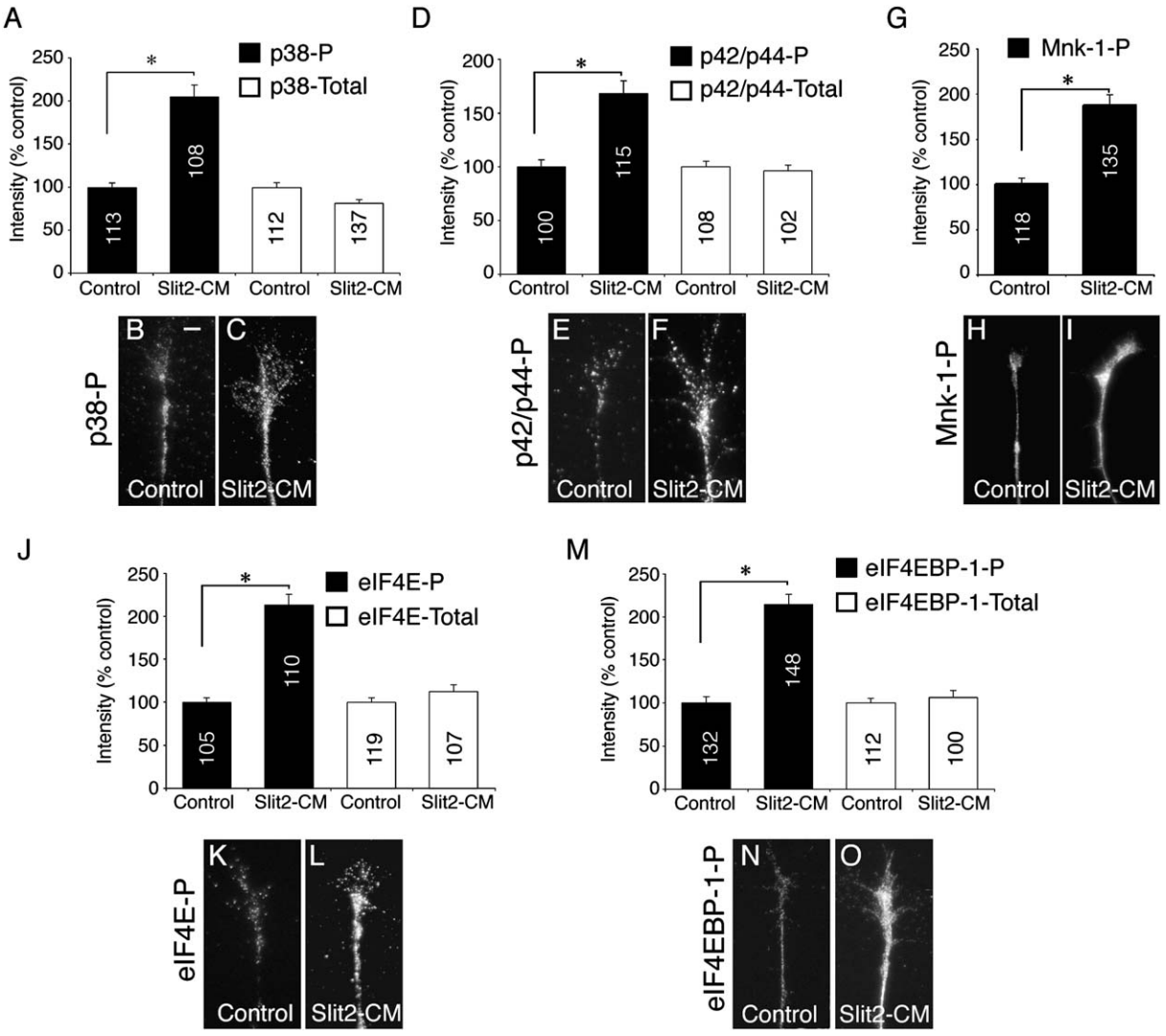

Figure 6. Rapid Activation of MAPKs and Translational Regulators

To assess the activation of MAPKs and translational regulators 5 min after Slit2-CM application, we used antibodies that specifically recognize the phosphorylated form of these proteins, coupled with digital quantitation of immunofluorescence. Slit2-CM caused a significant increase in phosphorylated p38 (p38-P) and phosphorylated p42/p44 (p42/p44-P) immunoreactivity when compared to controls (A–F). The immunoreactivity of total p38 and p42/p44 was not significantly altered. The level of phosphorylated Mnk-1 (Mnk-1-P) immunofluorescence within growth cones rose following application of Slit2-CM (G–I). The phosphorylated, but not total, forms of the transcriptional regulator eIF4E (J–L) and its binding protein eIF4EBP-1 (M–O) also displayed a significant increase in fluorescent signal intensity. Numbers inside bars denote growth cones tested. *$p < 0.001$, Kruskal-Wallis test (A, D, J, and M) or Mann-Whitney U test (G). Scale bar: 10 μm.

the translation initiation factor eIF4E within minutes of application to retinal growth cones.

Slit-Induced Decrease in Growth Cone F-Actin Depends on Protein Synthesis

As local PS is needed for chemotropic collapse induced by Slit2-CM, we wondered which mRNA species were being translated. A variety of mRNAs have been reported to be present in axonal growth cones, including many that encode proteins either forming or associating with the cytoskeleton, such as β-actin (Bassell et al., 1998), tau (Aronov et al., 2001), and actin-depolymerizing factor (ADF) (Lee and Hollenbeck, 2003). To identify mRNAs in *Xenopus* retinal growth cones, we cultured whole eyes from stage 24–30 embryos for 36 hr, then severed the retinal neurites. mRNA was extracted separately from the eyes and from the isolated axon/growth cones, and cDNA libraries were generated from these samples. Using PCR, we identified the glycolytic enzyme NADH dehydrogenase (NADHdh) in both the eye and axon/growth cone libraries, showing the mRNA extraction and cDNA synthesis to have been successful (Figure 7A). To assess the purity of the axon/growth cone preparation, PCR using primers against the cell body-specific histone H4 was performed. As can be seen in Figure 7A, only a very weak signal in the axon/growth cone lane is evident when compared to the eye lane after 30 PCR cycles, suggesting that there is little cell body contamination in this library.

Regulation of β-actin protein levels could provide one means of controlling growth cone cytoskeletal architecture. Using β-actin-specific primers, we identified

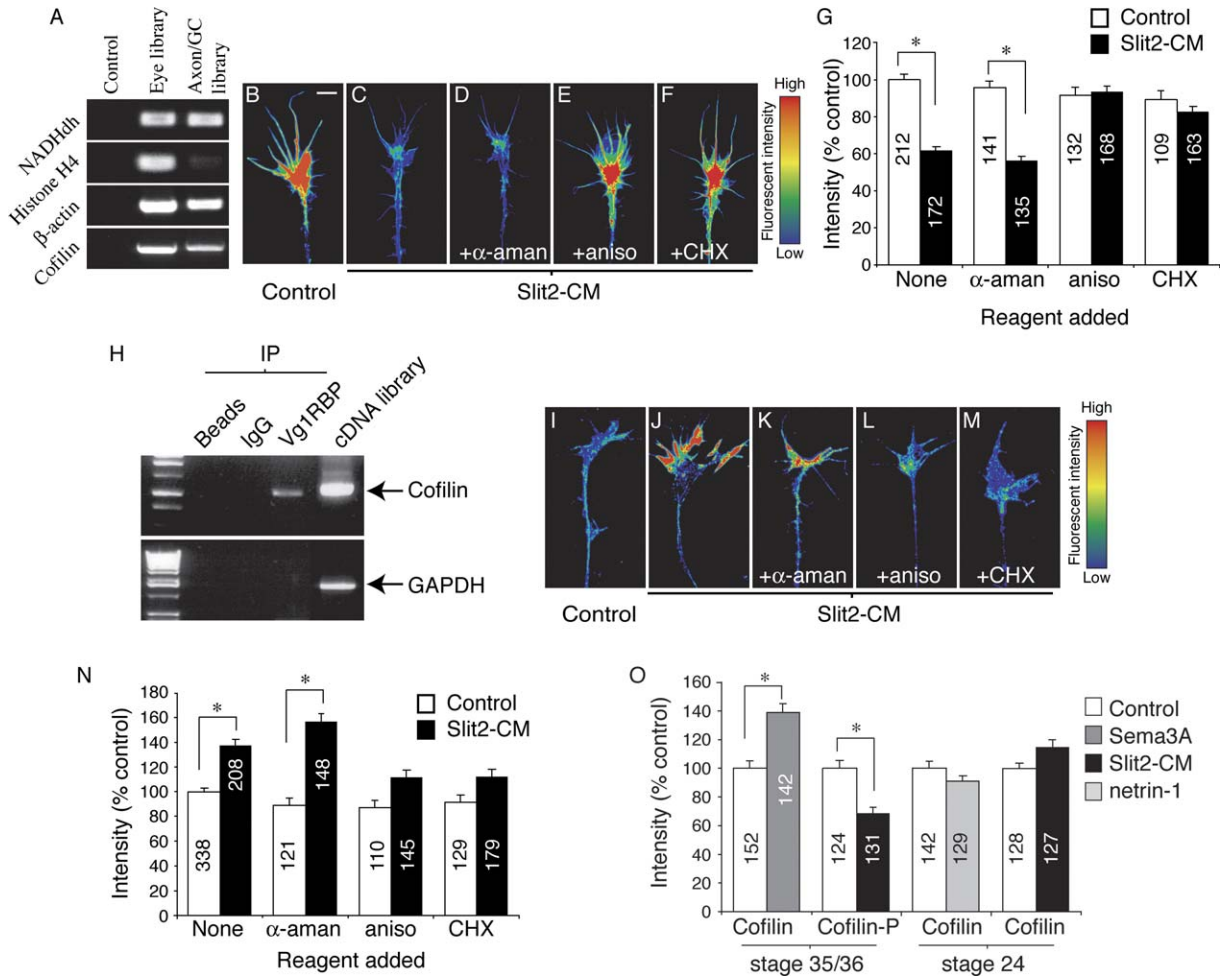

Figure 7. Slit-Induced Changes in Growth Cone F-Actin and Cofilin Are PS Dependent

cDNA libraries were constructed from mRNA extracted from cultured stage 35/36 eyes or isolated stage 35/36 cultured axons and growth cones. β-actin and cofilin were identified from both samples by using PCR (A). Using digital quantitation of immunofluorescence, Slit2-CM was shown to cause an ~40% decrease in growth cone F-actin fluorescent intensity (B, C, and G). This decrease was dependent on translation, but not transcription (D–G). Cofilin mRNA was immunoprecipitated with Vg1RBP bound to protein-A beads. Beads alone or beads coupled to rabbit IgG did not immunoprecipitate cofilin mRNA. GAPDH mRNA did not immunoprecipitate with Vg1RBP. *Xenopus* cDNA was used as a PCR positive control (H). Slit2-CM significantly raised total growth cone cofilin immunoreactivity after 5 min. This increase was not seen when translation was inhibited by aniso or CHX (I-N). Sema3A also elicited a rise in growth cone cofilin immunoreactivity, while phosphorylated cofilin (cofilin-P) immunofluorescence decreased in response to Slit2-CM. Cultured stage 24 growth cones stimulated with netrin-1 or Slit2-CM did not demonstrate a significant change in total cofilin fluorescent intensity (O). Numbers inside bars denote growth cones tested. Growth cone images have been pseudocolored to represent fluorescent intensity: low intensity, blue; high intensity, red. *$p < 0.001$, Kruskal-Wallis test. Scale bar: 5 μm.

β-actin cDNA in the axon/growth cone library (Figure 7A). To assess whether β-actin was being locally synthesized in response to Slit2-CM, we used digital quantitation of immunofluorescence by labeling with an antibody capable of recognizing both monomeric and polymerized β-actin. After 5 min, Slit2-CM caused a small but significant decrease in the fluorescent intensity of growth cone β-actin (control, 100% ± 1.68%; Slit2-CM, 93.2% ± 1.84%, $p < 0.001$ Mann-Whitney U test). As our data do not support a role for local proteasomal degradation in Slit2-CM-induced collapse, this effect may arise from an increased depolymerization of filamentous actin (F-actin), followed by transport of monomeric β-actin away from the growth cone. Consistent with this, previous studies have shown that brain-derived collapsing factor (Sema3A) elicits a rapid decrease in F-actin within chick dorsal root ganglion (DRG) growth cones in vitro (Fan et al., 1993). Using Alexa-phalloidin, we were able to detect a significant decrease (40% reduction of fluorescent intensity) in growth cone F-actin 5 min after addition of Slit2-CM. Importantly, the decrease in F-actin fluorescent intensity was dependent on PS, but not transcription, as the effect was blocked with aniso and CHX, but not α-aman (Figures 7B–7G).

Cofilin Is a Potential Target for Cue-Induced Local Translation

This finding led us to investigate the potential targets for local mRNA translation that could culminate in a reduction in growth cone F-actin. Inserts from 100 randomly selected colonies from the axon/growth cone cDNA library were sequenced and revealed a coding sequence for cofilin, an actin-depolymerizing protein homologous to vertebrate ADF (Abe et al., 1996). PCR

with cofilin-specific primers confirmed that cofilin cDNA was present in the library (Figure 7A). mRNA transcripts are transported to distant cytoplasmic compartments of neurons by RNA binding proteins (RBPs) (Agnes and Perron, 2004). *Xenopus* Vg1RBP, a homolog of the RNA binding protein zipcode binding protein (ZBP1), is highly expressed in developing RGCs, particularly in their axons and growth cones (F.vH. and C.H., unpublished data); thus, we next asked whether cofilin mRNA associates with this protein. Vg1RBP was immunoprecipitated from lysates of embryonic *Xenopus* heads by using a Vg1RBP antibody coupled to protein-A beads, followed by RNA extraction from the immunoprecipitate and RT-PCR with cofilin-specific primers. Cofilin RNA was detected in samples immunoprecipitated with Vg1RBP, but not those immunoprecipitated with uncoupled beads or rabbit IgG-coupled beads (Figure 7H). An interaction with Vg1RBP and GAPDH was not seen, suggesting the interaction with cofilin may be specific (Figure 7H). Thus, our results provide evidence that cofilin mRNA binds to Vg1RBP1. Whether this association is required for transport and localization to retinal growth cones remains to be determined.

To investigate whether cofilin is locally synthesized in response to guidance cues, we bath-applied Slit2-CM to retinal cultures for 5 min, then assayed total levels of growth cone cofilin immunofluorescence. Slit2-CM elicited an ~33% increase in cofilin fluorescent intensity, and importantly, this effect was dependent on PS, as the Slit2-CM-induced rise in growth cone cofilin signal intensity was not observed when translation was inhibited with CHX or aniso (Figures 7I–7N).

We then used another repellent that causes PS-dependent collapse, Sema3A, to investigate whether cofilin upregulation is common during collapse. Sema3A also stimulated a marked elevation in cofilin fluorescent intensity in retinal growth cones after 5 min, suggesting a common link between PS-dependent collapse and a rise in growth cone cofilin (Figure 7O). Cofilin is also regulated posttranslationally via phosphorylation, which renders it incapable of binding and depolymerizing F-actin (Arber et al., 1998). After 5 min stimulation with Slit2-CM, the fluorescent intensity of phosphorylated cofilin (cofilin-P) was significantly lower than controls (Figure 7O). Together with the potential increase through PS, this could culminate in a larger pool of active cofilin in comparison to controls. To further investigate the link between elevated cofilin and collapse, we repeated these experiments with the use of cultured stage 24 retinal explants, which do not collapse in response to Slit2-CM (Figure 1K). Five minutes after addition of Slit2-CM, quantitation of total cofilin immunofluorescence in these retinal growth cones showed that the signal intensity of cofilin was not altered significantly (Figure 7O). However, this may be due to growth cones of this age being unresponsive toward this repellent. To address this, we cultured stage 24 explants on a fibronectin substrate and stimulated them with netrin-1. Under these conditions, netrin-1 acts as an attractant for cultured retinal axons (Shewan et al., 2002). The signal intensity of growth cone cofilin was not significantly changed 5 min after addition of netrin-1, implying that a local, PS-dependent increase in cofilin may be causally related to collapse. Initial experiments using a variety of antisense oligonucleotides have as yet proven unsuccessful in specifically inhibiting local cue-induced cofilin translation, thus requiring future experimentation to verify this.

Discussion

Our results show that Slit2-CM activates MAPKs and translation regulators in retinal growth cones, leading to chemotropic collapse. Local translation and endocytosis are required to elicit this response, and disruption of HS inhibits PS and collapse. Intriguingly, growth cone F-actin immunoreactivity declines rapidly in response to Slit2-CM, while cofilin immunoreactivity increases, and these changes depend on local PS. The possibility of local cofilin translation contributing to cytoskeletal remodelling is supported by the presence of cofilin transcripts in retinal axons. Together our data suggest a model whereby Slit/Robo binding leads to local PS, perhaps of the actin depolymerizing factor cofilin, followed by cytoskeletal rearrangements through depolymerization of F-actin, and growth cone collapse.

Both Slit2 and Robo2 are involved in multiple aspects of RGC axon guidance. Robo2 is expressed in RGCs of the retina, and zebrafish *astray* mutants display aberrant RGC axon trajectories, including inappropriate defasciculation and abnormal axonal projections both anteriorly into the diencephalon and posteriorly into the hindbrain (Fricke et al., 2001; Hutson and Chien, 2002). Similarly, in mammalian retinal axon guidance, Slit2 has been shown to mediate axonal behavior at key intermediate targets, such as the optic chiasm (Erskine et al., 2000; Plump et al., 2002) and the diencephalon (Ringstedt et al., 2000). The expression of Robo2 within the developing RGCs and of Slit along the dorsomedial, anterior, and posterior borders of the optic tectum of stage 40 *Xenopus* embryos is consistent with a role for these molecules in regulating axonal behavior at a later stage in RGC axon pathfinding. We postulate that Slit expression allows for "surround repulsion," as has been described for spinal sensory axons (Keynes et al., 1997), preventing RGC axons from leaving the tectum anteriorly, dorsally, or posteriorly.

Our finding that HS sidechains are involved in PS and collapse triggered by Slit2-CM may also be relevant to this hypothesis. HSs have been shown to modulate responses to guidance cues such as FGF-2 (Walz et al., 1997) and Sema5A (Kantor et al., 2004). With respect to the retinotectal projection, HSPG synthesis is required for axon sorting en route to the tectum, as mutations to the zebrafish *ext2* and *etx3* genes, which encode glycosyltransferases essential for HSPG biosynthesis, result in missorting in the optic tract (Lee et al., 2004b). Furthermore, HSs, particularly 6-*O*-sulfated HSs, have previously been shown to be essential for retinal axon targeting, and the enzymes responsible for 2-*O*- or 6-*O*-sulfation, HS 2-*O*-sulfotransferase and HS 6-*O*-sulfotransferase, are expressed around the optic pathway and in the posterior tectum (Irie et al., 2002). Biochemical studies have also suggested that *O*-sulfate groups on the HSPG glypican-1 are essential for high-affinity binding to Slit2 (Ronca et al., 2001). This implies that *O*-sulfated HSPGs may modulate the activity of Slit to control axonal navigation in the region of the tectum. Indeed, interfering with HSs in vivo causes retinal axons

to inappropriately invade Slit-expressing areas, such as the dorsal midline (Irie et al., 2002). Further work will be required to determine which HS chains regulate Slit/Robo2 interactions.

We also find that clathrin-mediated endocytosis is required for collapse induced by Slit2-CM. Although the precise role this plays in RGC growth cone responses is currently unclear, endocytosis may be pertinent to many aspects of axonal navigation. Sema3A induces rapid endocytosis from the surface of embryonic DRG growth cones in vitro (Jurney et al., 2002) and causes neuropilin-1 and plexin, the Sema3A receptors, to partition into cytoplasmic vacuoles (Fournier et al., 2000). We have also recently shown that Sema3A and netrin-1 can cause a rapid endocytosis-dependent decrease in the surface expression of their respective receptors, neuropilin-1 and DCC (Piper et al., 2005). Endocytosis of receptors may enable growth cones to rapidly attenuate their responsiveness, the subsequent desensitization forming part of an adaptation response that enables growth cones to continually adjust their sensitivity to environmental cues. Endocytosis may also play a more central role in signal transduction, as signaling from endocytosed receptors can continue from internalized compartments (Di Guglielmo et al., 2003; Hayes et al., 2002). Indeed, the activity of MAPKs is suppressed in some cells incapable of performing endocytosis (Vieira et al., 1996). The withdrawal of filopodia and lamellipodia seen in collapsing growth cones may also be dependent on endocytosis. Internalization of cell adhesion molecules such as L1 (Castellani et al., 2004; Kamiguchi and Yoshihara, 2001) after application of a guidance cue may represent a mechanism to decrease adherence to the substrate, and endocytosis may also enable retrieval and recycling of plasma membrane from the receding axon tip (Zakharenko and Popov, 2000).

Our findings suggest that signal transduction occurs via the p38 and p42/p44 MAPK pathways, and furthermore implicate Slit2-CM-induced local PS in the process of cytoskeletal remodelling. Axonal PS has been described in numerous invertebrate and vertebrate neurons (Alvarez et al., 2000; Piper and Holt, 2004) and may play a role in such diverse events as synaptic potentiation (Zhang and Poo, 2002), axonal regeneration (Zheng et al., 2001), and long-term facilitation (Casadio et al., 1999; Martin et al., 1997). Furthermore, in *Xenopus* growth cones, local PS is necessary for the directional response of axons to the guidance factors Sema3A and netrin-1 in vitro (Campbell and Holt, 2001) and in the process of resensitization to cues such as netrin-1 (Ming et al., 2002; Piper et al., 2005). Our finding that Slit2-CM elicits a PS-dependent reduction in growth cone F-actin fluorescent intensity provides another potential role for axonal PS: the regulation of cytoskeletal dynamics through rapid synthesis of proteins capable of remodelling the actin cytoskeleton.

Furthermore, the finding that cofilin immunoreactivity markedly increases in growth cones in response to both Slit2-CM and Sema3A suggests the intriguing idea that the local synthesis of actin-depolymerizing proteins contributes to repellent-induced collapse. Cofilin, a member of the ADF/cofilin family of actin-depolymerizing molecules (Sarmiere and Bamburg, 2004), is a small protein of ~19 kDa, and its mRNA and protein have been detected in a variety of neuronal axons and growth cones (Lee and Hollenbeck, 2003; Willis et al., 2005). Importantly, in vitro experiments have previously implicated ADF/cofilin in the control of chick retinal growth cone filopodial dynamics in response to brain-derived neurotrophic factor (Gehler et al., 2004), and moreover, axons of cultured rat DRG axons have been shown to synthesize cofilin 1 (Willis et al., 2005). However, our data provide a potential link between cue-induced growth cone behavior and local cofilin translation. Two *Xenopus* cofilin proteins have been reported, and their high level of identity at the amino acid level suggests that they are allelic variants, as *Xenopus* has a tetraploid genome (Abe et al., 1996). Locally controlling their synthesis may provide one means of influencing the balance of actin stability; in the case of Slit, perhaps resulting in an increase in growth cone cofilin and a subsequent shift toward actin depolymerization and hence growth cone collapse. This may also be consistent with respect to recent reports linking cofilin activity to shrinkage of dendritic spines in long-term synaptic depression (Zhou et al., 2004) and axon growth and neuronal morphogenesis (Ng and Luo, 2004). The idea that the mRNAs of cytoskeletal regulators are key targets for cue-induced translation is in line with recent evidence demonstrating that local synthesis of the small GTPase RhoA is necessary for Sema3A-induced collapse in mammalian sensory growth cones (Wu et al., 2005).

Our data also suggest that regulation of cofilin in response to Slit also occurs at a posttranslational level, as Slit2-CM caused a significant decrease in the growth cone signal intensity of phosphorylated cofilin. A similar phenomenon has been reported for Sema3A, which induces a rapid (1 min) increase in phospho-cofilin in embryonic murine DRG neurons, followed by a dramatic decrease after 5 min (Aizawa et al., 2001). This suggests that a cycle of inactivation/activation of cofilin, regulated by kinases such as LIM-kinase and phosphatases such as Slingshot (Ng and Luo, 2004) may play a role in collapse. This may also be related to calcium (Ca^{2+}) signaling, as high levels of focally released caged Ca^{2+} activate calcium-calmodulin-dependent protein kinase II (CaMKII) to induce growth cone attraction, while lower levels cause repulsion via a mechanism involving phosphatases such as calcineurin (CaN) (Wen et al., 2004). Furthermore, in vitro cell culture studies have shown that the phosphatase responsible for dephosphorylating cofilin, Slingshot, is activated in a Ca^{2+}/CaN-dependent fashion (Wang et al., 2005). Thus, Slit may increase the local actin-severing activity of cofilin in growth cones by triggering two parallel mechanisms—local synthesis of new cofilin and dephosphorylation of existing cofilin—that act in concert to promote changes in the cytoskeleton.

Much remains to be defined with regard to how cofilin mRNA is transported and localized in *Xenopus* retinal growth cones. Developing neurons express many RBPs, which play roles not just in transporting mRNA but also in regulating their translation. For example, transcripts are "silenced" during transport and are kept silent at their specific destinations until needed (Agnes and Perron, 2004). Our data show that cofilin mRNA associates with Vg1RBP (a homolog of ZPB1) and suggest that this protein may regulate its transport to the growth

cones and possibly its translational state. The RBP ZBP1 is known to bind to β-actin mRNA through a conserved sequence in the 3′ untranslated region (UTR) known as the zipcode. This association is required for the localization of β-actin mRNA to the growth cones of cultured chick retinal neurons (Zhang et al., 2001). However, the 3′ UTR of *Xenopus* cofilin mRNA does not possess a recognizable zipcode, indicating that its association with Vg1RBP may be mediated via an alternative region or through a structural motif in the mRNA.

While our data suggest that cofilin levels may increase 5 min after Slit2-CM addition in a PS-dependent manner, local translation of cofilin is not the only plausible explanation for this finding. We cannot rule out the possibility that other proteins are translated in the growth cone, which are subsequently involved in promoting the transport of cofilin into the growth cone. Future studies aimed at specifically blocking translation of cofilin mRNA will help resolve this issue and will clarify whether local cofilin synthesis is causally related to collapse. In summary, our data provide an insight into how Slit2 may mediate growth cone guidance in RGC growth cones, highlighting the roles of HS, endocytosis, activation of the p38 and p42/p44 MAPK pathways, and local PS. We speculate that in an in vivo context, such as when RGC axons reach the dorsal margins of the *Xenopus* tectum, local encounters with this cue may lead to the concomitant synthesis of new cofilin and dephosphorylation of existing cofilin, which elicits actin depolymerization and results in growth cone retraction and confinement to the tectum.

Experimental Procedures

Embryos

Xenopus laevis embryos were in vitro fertilized, raised in 0.1X Modified Barth's Saline at 14ºC–20ºC, and staged by the tables of Nieuwkoop and Faber.

Slit2 Expression

HEK cells stably transfected with hSlit2 (a *Xenopus* Slit homolog) carrying a C-terminal *myc* tag or the parental control plasmid (provided by Y. Rao) were cultured for 48 hr prior to collection of conditioned medium. A Western blot with a monoclonal anti-*myc* antibody showed a major band at ~200 kDa in Slit2-CM, corresponding to full-length Slit2, and another at ~55–60 kDa, likely representing the C-terminal product arising from proteolytic cleavage of the parent protein. No bands were seen in the control conditioned medium. A dose/response curve was generated by using Slit2-CM in collapse assays using 24 hr cultures of stage 35/36 retinal explants. The lowest dose that consistently caused maximal collapse was one part Slit2-CM to four parts culture medium. This dose was used for collapse, ^{3}H-leucine incorporation, and quantitative immunohistochemistry assays.

In Situ Hybridization

Visualization of the optic tract was performed using horseradish peroxidase type VI and diaminobenzidine (Sigma) (Cornel and Holt, 1992). In situ hybridization was performed as described previously (Campbell et al., 2001).

Retinal Cultures

Eye primordia were dissected from stage 24, 28, 32, 35/36, or 40 embryos and cultured at 20ºC for 24 hr on coverslips coated with 10 μg/ml poly-L-lysine (Sigma) and 10 μg/ml laminin (Sigma) or 1 μg/ml fibronectin (Sigma; for stage 24 cultures stimulated with netrin-1).

Collapse Assays

Slit2-CM or control was added per well at a dilution of 1:4. After 10 min, cultures were fixed in 2% PFA + 7.5% sucrose, then the number of collapsed growth cones was counted. Values are presented as percentage of growth cone collapse ± SEM. Statistical analyses were performed using a two-tailed Mann-Whitney U test.

Growth Cone Turning Assay

Eight-hundred μl of Slit2-CM (or control) was concentrated to 50 μl with the use of a centrifugal filter. Five μl was then mixed with 35 μl of culture medium for use in the assay. Gradients of diffusible Slit2-CM protein (or control) were established by ejecting the sample out of a micropipette with a tip opening of 1 μm. Growth cones from 24 hr cultures of stage 35/36 retinal explants were positioned 100 μm from the tip opening at an angle of 45º relative to the initial direction of the axon shaft and observed at 20X. Pictures were taken every 10 min for 1 hr. Turning angles were measured using Open*lab* software (Improvision). Statistical analysis was performed using a two-tailed t test.

Pharmacological Agents

Immediately prior to the addition of Slit2-CM in collapse assays, the following reagents were bath-applied to retinal cultures: 10 μg/ml α-aman (Calbiochem); 25 μM CHX (Sigma); 40 μM aniso (Sigma); 50 μM N-Acetyl-Leu-Leu-NorLeu-Al (LLnL, Sigma); 10 μM lacta (Sigma); 10 nM rapa (Calbiochem); 50 nM wort (Biomol); 50 μM PAO (Sigma); 100 nM MDC (Sigma); 25 μM PD98059 (Calbiochem); 10 μM U0126 (Calbiochem); 25 μM SB203580 (Calbiochem). H'ase I (2.5 U/ml, Sigma) and C'ase ABC (0.25 or 1.0 U/ml, Sigma) were added 3 hr prior to collapse assays being performed.

^{3}H-Leucine Incorporation Assay

To measure PS in isolated axons and growth cones, incorporation of L-[4,5-^{3}H]-leucine (5.66 TBq/mmol; Amersham) followed by protein precipitation with TCA was used (Campbell and Holt, 2001). Twenty-four hr cultures of stage 35/36 explants were grown, taking care to ensure similar amounts of explant tissue per coverslip. Explants were removed by cutting free from the neurites. Coverslips with adherent growth cones were transferred to leucine-free medium and randomly assigned to treatment groups. Inhibitors were added 5 min prior to addition of L-[4,5-^{3}H]-leucine, after which Slit2-CM or control supernatant was added. After 10 min, cultures were rinsed and fixed in 25% TCA for 30 min. ^{3}H uptake was measured with a scintillation counter. Duplicates were included in each experiment. Data are presented as a percentage of the ^{3}H-leucine uptake in the control sample ± SEM. Statistical analyses were performed using analysis of variance (Kruskal-Wallis with post-test).

Antibodies

Antibodies against the phosphorylated and/or total forms of the following proteins were obtained from Cell Signaling Technology: Mnk-1, p42/p44, p38, eIF4E, and eIF4EBP-1. These antibodies were used at 1:100. The labeling observed by the phosphorylated antibodies Mnk-1-P, p42/p44-P, eIF4E-P, and eIF4EBP-1-P was blocked by preincubation with their respective phospho-peptides (data not shown). F-actin was visualized with Alexa-Fluor 594-phalloidin (used at 1:40; Molecular Probes). Antibodies against cofilin and cofilin-P were kindly provided by J. Bamburg and were used at 1:200.

Quantitation of Fluorescence Intensity

Twenty-four hr cultures of stage 35/36 retinal explants were incubated with Slit2-CM or control for 5 min, fixed in 2% paraformaldehyde/7.5% sucrose, permeabilized with 0.1% Triton X-100, blocked in 10% goat serum, then labeled with primary antibodies and Cy3 secondary antibodies (1:700, Chemicon) for 1 hr each, and mounted in FluorSave (Calbiochem). Noncollapsed growth cones were visualized at 100× on a Nikon Optiphot inverted microscope. Using phase optics to avoid biased selection of fluorescence, a growth cone was randomly selected and imaged using a Hamamatsu digital CCD camera. A fluorescent image was then captured, exposure time being kept constant and below greyscale pixel saturation. For quantitation of fluorescence intensity, the growth cone outline was traced on the phase image by using Open*lab* software (Improvision), then superimposed on the fluorescent image. The software calculated

the fluorescent intensity within the growth cone, giving a measurement of pixel intensity per unit area. The growth cone outline was then placed in an adjacent area clear of cellular material to record the background fluorescent intensity. This reading was subtracted from the growth cone reading, yielding the background-corrected intensity. The fluorescent intensities of between 25 to 40 growth cones per sample group in each experiment were collected. Data were normalized against the control-treated groups to allow for comparisons between experiments and are presented as percentage of control fluorescent intensity ± SEM. Samples from independent experiments were stained, imaged, and processed under identical conditions. Counts in which the experimenter was blind to the identity of samples resulted in similar results. Statistical analyses were performed using analysis of variance (Kruskal-Wallis with post-test) or a two-tailed Mann-Whitney U test (Figure 6G).

Axon/Growth Cone Library

Sixty eye primordia from stage 24–30 *Xenopus* embryos were cultured for 36 hr on precoated coverslips (see above). Axons were severed with a fine steel pin, and the eye explants were removed. The axons/growth cones adhering to the plastic were solubilized and RNA was extracted (Absolutely RNA Nanoprep Kit, Stratagene). cDNA was synthesized using the Super SMART PCR cDNA Synthesis Kit (Clontech). The cDNA was amplified using primers containing the "SMART" sequence. Fragments larger than 1 kb were gel-purified using the QIAquick Gel Extraction Kit (Qiagen), ligated to the pGEM-T Easy vector (Promega), and transfected into competent *E. coli* (DH5α). Colony PCR was performed using primers complementary to the vector and sequenced by Lark using a primer complementary to the T7 promoter.

Immunoprecipitation and Cofilin mRNA Detection

Analysis of Vg1RBP and cofilin mRNA interaction was performed as described (Gu et al., 2002), with minor modifications. Heads of stage 35/36 *Xenopus* embryos were lysed in RIPA buffer. After centrifugation, lysates were incubated with 5 μg/ml rabbit IgG coupled to protein A-coupled sepharose beads (Amersham) for 30 min at 4ºC. Precleared lysates were incubated with protein A beads, protein A beads coupled to 5 μg/ml rabbit IgG or 15 μl Vg1RBP antiserum (a gift from N. Standart) for 1 hr at 4ºC with gentle agitation. To detect cofilin and GAPDH mRNA, the pelleted sepharose beads were washed well with PBS containing 300 mM NaCl, resuspended in 100 μl water, and treated with DNase for 15 min at 37ºC. Total RNA was extracted using Trizol RNA isolation reagent (Invitrogen) and used as a template in the RT-PCR reaction using ReadyToGo RT-PCR beads (Amersham). PCR was performed for 30 cycles with the primers specific for cofilin and GAPDH mRNA. cDNA generated from stage 32 *Xenopus* embryos was used as the PCR positive control.

Statistics

Statistical analyses were performed using Graphpad InStat3. Each experiment was conducted independently a minimum of four times.

Acknowledgments

We thank D. Campbell and B. Harris for helpful discussions; and V. Nurcombe, C-B. Chien, J. Bamburg, N. Standart, and Y. Rao for reagents. We are grateful to D. O'Connor, D. Pask, S. Shipway, S. Diamantakis, S. Cordiner-Lawrie, A. Bowden, and A. Curry for technical assistance. This work was funded by a Wellcome Trust Programme grant (C.H.), an EMBO long-term fellowship (F.v.H.), a C J Martin Fellowship (R.A.), and a Croucher Foundation Scholarship (K.M.L.).

Received: May 4, 2005
Revised: September 23, 2005
Accepted: December 5, 2005
Published: January 18, 2006

References

Abe, H., Obinata, T., Minamide, L.S., and Bamburg, J.R. (1996). Xenopus laevis actin-depolymerizing factor/cofilin: a phosphorylation-regulated protein essential for development. J. Cell Biol. *132*, 871–885.

Agnes, F., and Perron, M. (2004). RNA-binding proteins and neural development: a matter of targets and complexes. Neuroreport *15*, 2567–2570.

Aizawa, H., Wakatsuki, S., Ishii, A., Moriyama, K., Sasaki, Y., Ohashi, K., Sekine-Aizawa, Y., Sehara-Fujisawa, A., Mizuno, K., Goshima, Y., et al. (2001). Phosphorylation of cofilin by LIM-kinase is necessary for semaphorin 3A-induced growth cone collapse. Nat. Neurosci. *4*, 367–373.

Alvarez, J., Giuditta, A., and Koenig, E. (2000). Protein synthesis in axons and terminals: significance for maintenance, plasticity and regulation of phenotype. With a critique of slow transport theory. Prog. Neurobiol. *62*, 1–62.

Arber, S., Barbayannis, F.A., Hanser, H., Schneider, C., Stanyon, C.A., Bernard, O., and Caroni, P. (1998). Regulation of actin dynamics through phosphorylation of cofilin by LIM-kinase. Nature *393*, 805–809.

Aronov, S., Aranda, G., Behar, L., and Ginzburg, I. (2001). Axonal tau mRNA localization coincides with tau protein in living neuronal cells and depends on axonal targeting signal. J. Neurosci. *21*, 6577–6587.

Bashaw, G.J., Kidd, T., Murray, D., Pawson, T., and Goodman, C.S. (2000). Repulsive axon guidance: Abelson and Enabled play opposing roles downstream of the roundabout receptor. Cell *101*, 703–715.

Bassell, G.J., Zhang, H., Byrd, A.L., Femino, A.M., Singer, R.H., Taneja, K.L., Lifshitz, L.M., Herman, I.M., and Kosik, K.S. (1998). Sorting of beta-actin mRNA and protein to neurites and growth cones in culture. J. Neurosci. *18*, 251–265.

Bulow, H.E., and Hobert, O. (2004). Differential sulfations and epimerization define heparan sulfate specificity in nervous system development. Neuron *41*, 723–736.

Campbell, D.S., and Holt, C.E. (2001). Chemotropic responses of retinal growth cones mediated by rapid local protein synthesis and degradation. Neuron *32*, 1013–1026.

Campbell, D.S., Regan, A.G., Lopez, J.S., Tannahill, D., Harris, W.A., and Holt, C.E. (2001). Semaphorin 3A elicits stage-dependent collapse, turning, and branching in Xenopus retinal growth cones. J. Neurosci. *21*, 8538–8547.

Casadio, A., Martin, K.C., Giustetto, M., Zhu, H., Chen, M., Bartsch, D., Bailey, C.H., and Kandel, E.R. (1999). A transient, neuron-wide form of CREB-mediated long-term facilitation can be stabilized at specific synapses by local protein synthesis. Cell *99*, 221–237.

Castellani, V., Falk, J., and Rougon, G. (2004). Semaphorin3A-induced receptor endocytosis during axon guidance responses is mediated by L1 CAM. Mol. Cell. Neurosci. *26*, 89–100.

Cornel, E., and Holt, C. (1992). Precocious pathfinding: retinal axons can navigate in an axonless brain. Neuron *9*, 1001–1011.

Di Guglielmo, G.M., Le Roy, C., Goodfellow, A.F., and Wrana, J.L. (2003). Distinct endocytic pathways regulate TGF-beta receptor signalling and turnover. Nat. Cell Biol. *5*, 410–421.

Dickson, B.J. (2002). Molecular mechanisms of axon guidance. Science *298*, 1959–1964.

Erskine, L., Williams, S.E., Brose, K., Kidd, T., Rachel, R.A., Goodman, C.S., Tessier-Lavigne, M., and Mason, C.A. (2000). Retinal ganglion cell axon guidance in the mouse optic chiasm: expression and function of robos and slits. J. Neurosci. *20*, 4975–4982.

Fan, J., Mansfield, S.G., Redmond, T., Gordon-Weeks, P.R., and Raper, J.A. (1993). The organization of F-actin and microtubules in growth cones exposed to a brain-derived collapsing factor. J. Cell Biol. *121*, 867–878.

Fan, X., Labrador, J.P., Hing, H., and Bashaw, G.J. (2003). Slit stimulation recruits Dock and Pak to the roundabout receptor and increases Rac activity to regulate axon repulsion at the CNS midline. Neuron *40*, 113–127.

Fournier, A.E., Nakamura, F., Kawamoto, S., Goshima, Y., Kalb, R.G., and Strittmatter, S.M. (2000). Semaphorin3A enhances endocytosis at sites of receptor-F-actin colocalization during growth cone collapse. J. Cell Biol. *149*, 411–422.

Fricke, C., Lee, J.S., Geiger-Rudolph, S., Bonhoeffer, F., and Chien, C.B. (2001). astray, a zebrafish roundabout homolog required for retinal axon guidance. Science *292*, 507–510.

Gehler, S., Shaw, A.E., Sarmiere, P.D., Bamburg, J.R., and Letourneau, P.C. (2004). Brain-derived neurotrophic factor regulation of retinal growth cone filopodial dynamics is mediated through actin depolymerizing factor/cofilin. J. Neurosci. *24*, 10741–10749.

Gu, W., Pan, F., Zhang, H., Bassell, G.J., and Singer, R.H. (2002). A predominantly nuclear protein affecting cytoplasmic localization of beta-actin mRNA in fibroblasts and neurons. J. Cell Biol. *156*, 41–51.

Hayes, S., Chawla, A., and Corvera, S. (2002). TGF beta receptor internalization into EEA1-enriched early endosomes: role in signaling to Smad2. J. Cell Biol. *158*, 1239–1249.

Hu, H. (2001). Cell-surface heparan sulfate is involved in the repulsive guidance activities of Slit2 protein. Nat. Neurosci. *4*, 695–701.

Hutson, L.D., and Chien, C.B. (2002). Pathfinding and error correction by retinal axons: the role of astray/robo2. Neuron *33*, 205–217.

Irie, A., Yates, E.A., Turnbull, J.E., and Holt, C.E. (2002). Specific heparan sulfate structures involved in retinal axon targeting. Development *129*, 61–70.

Johnson, K.G., Ghose, A., Epstein, E., Lincecum, J., O'Connor, M.B., and Van Vactor, D. (2004). Axonal heparan sulfate proteoglycans regulate the distribution and efficiency of the repellent slit during midline axon guidance. Curr. Biol. *14*, 499–504.

Jurney, W.M., Gallo, G., Letourneau, P.C., and McLoon, S.C. (2002). Rac1-mediated endocytosis during ephrin-A2- and semaphorin 3A-induced growth cone collapse. J. Neurosci. *22*, 6019–6028.

Kamiguchi, H., and Yoshihara, F. (2001). The role of endocytic l1 trafficking in polarized adhesion and migration of nerve growth cones. J. Neurosci. *21*, 9194–9203.

Kantor, D.B., Chivatakarn, O., Peer, K.L., Oster, S.F., Inatani, M., Hansen, M.J., Flanagan, J.G., Yamaguchi, Y., Sretavan, D.W., Giger, R.J., et al. (2004). Semaphorin 5A is a bifunctional axon guidance cue regulated by heparan and chondroitin sulfate proteoglycans. Neuron *44*, 961–975.

Keynes, R., Tannahill, D., Morgenstern, D.A., Johnson, A.R., Cook, G.M., and Pini, A. (1997). Surround repulsion of spinal sensory axons in higher vertebrate embryos. Neuron *18*, 889–897.

Kidd, T., Bland, K.S., and Goodman, C.S. (1999). Slit is the midline repellent for the robo receptor in Drosophila. Cell *96*, 785–794.

Lee, H., Engel, U., Rusch, J., Scherrer, S., Sheard, K., and Van Vactor, D. (2004a). The microtubule plus end tracking protein Orbit/MAST/CLASP acts downstream of the tyrosine kinase Abl in mediating axon guidance. Neuron *42*, 913–926.

Lee, J.S., von der Hardt, S., Rusch, M.A., Stringer, S.E., Stickney, H.L., Talbot, W.S., Geisler, R., Nusslein-Volhard, C., Selleck, S.B., Chien, C.B., et al. (2004b). Axon sorting in the optic tract requires HSPG synthesis by ext2 (dackel) and extl3 (boxer). Neuron *44*, 947–960.

Lee, S.K., and Hollenbeck, P.J. (2003). Organization and translation of mRNA in sympathetic axons. J. Cell Sci. *116*, 4467–4478.

Long, H., Sabatier, C., Ma, L., Plump, A., Yuan, W., Ornitz, D.M., Tamada, A., Murakami, F., Goodman, C.S., and Tessier-Lavigne, M. (2004). Conserved roles for Slit and Robo proteins in midline commissural axon guidance. Neuron *42*, 213–223.

Lundstrom, A., Gallio, M., Englund, C., Steneberg, P., Hemphala, J., Aspenstrom, P., Keleman, K., Falileeva, L., Dickson, B.J., and Samakovlis, C. (2004). Vilse, a conserved Rac/Cdc42 GAP mediating Robo repulsion in tracheal cells and axons. Genes Dev. *18*, 2161–2171.

Mann, F., Miranda, E., Weinl, C., Harmer, E., and Holt, C.E. (2003). B-type Eph receptors and ephrins induce growth cone collapse through distinct intracellular pathways. J. Neurobiol. *57*, 323–336.

Martin, K.C., Casadio, A., Zhu, H., Yaping, E., Rose, J.C., Chen, M., Bailey, C.H., and Kandel, E.R. (1997). Synapse-specific, long-term facilitation of aplysia sensory to motor synapses: a function for local protein synthesis in memory storage. Cell *91*, 927–938.

Ming, G.L., Wong, S.T., Henley, J., Yuan, X.B., Song, H.J., Spitzer, N.C., and Poo, M.M. (2002). Adaptation in the chemotactic guidance of nerve growth cones. Nature *417*, 411–418.

Ng, J., and Luo, L. (2004). Rho GTPases regulate axon growth through convergent and divergent signaling pathways. Neuron *44*, 779–793.

Niclou, S.P., Jia, L., and Raper, J.A. (2000). Slit2 is a repellent for retinal ganglion cell axons. J. Neurosci. *20*, 4962–4974.

Piper, M., and Holt, C. (2004). RNA translation in axons. Annu. Rev. Cell Dev. Biol. *20*, 505–523.

Piper, M., Salih, S., Weinl, C., Holt, C.E., and Harris, W.A. (2005). Endocytosis-dependent desensitization and protein synthesis-dependent resensitization in retinal growth cone adaptation. Nat. Neurosci. *8*, 179–186.

Plump, A.S., Erskine, L., Sabatier, C., Brose, K., Epstein, C.J., Goodman, C.S., Mason, C.A., and Tessier-Lavigne, M. (2002). Slit1 and Slit2 cooperate to prevent premature midline crossing of retinal axons in the mouse visual system. Neuron *33*, 219–232.

Raught, B., and Gingras, A.C. (1999). eIF4E activity is regulated at multiple levels. Int. J. Biochem. Cell Biol. *31*, 43–57.

Ray, E., and Samanta, A.K. (1996). Dansyl cadaverine regulates ligand induced endocytosis of interleukin-8 receptor in human polymorphonuclear neutrophils. FEBS Lett. *378*, 235–239.

Ringstedt, T., Braisted, J.E., Brose, K., Kidd, T., Goodman, C., Tessier-Lavigne, M., and O'Leary, D.D. (2000). Slit inhibition of retinal axon growth and its role in retinal axon pathfinding and innervation patterns in the diencephalon. J. Neurosci. *20*, 4983–4991.

Ronca, F., Andersen, J.S., Paech, V., and Margolis, R.U. (2001). Characterization of Slit protein interactions with glypican-1. J. Biol. Chem. *276*, 29141–29147.

Sarmiere, P.D., and Bamburg, J.R. (2004). Regulation of the neuronal actin cytoskeleton by ADF/cofilin. J. Neurobiol. *58*, 103–117.

Shewan, D., Dwivedy, A., Anderson, R., and Holt, C.E. (2002). Age-related changes underlie switch in netrin-1 responsiveness as growth cones advance along visual pathway. Nat. Neurosci. *5*, 955–962.

Steigemann, P., Molitor, A., Fellert, S., Jackle, H., and Vorbruggen, G. (2004). Heparan sulfate proteoglycan syndecan promotes axonal and myotube guidance by slit/robo signaling. Curr. Biol. *14*, 225–230.

Vieira, A.V., Lamaze, C., and Schmid, S.L. (1996). Control of EGF receptor signaling by clathrin-mediated endocytosis. Science *274*, 2086–2089.

Walz, A., McFarlane, S., Brickman, Y.G., Nurcombe, V., Bartlett, P.F., and Holt, C.E. (1997). Essential role of heparan sulfates in axon navigation and targeting in the developing visual system. Development *124*, 2421–2430.

Wang, Y., Shibasaki, F., and Mizuno, K. (2005). Calcium signal-induced cofilin dephosphorylation is mediated by Slingshot via calcineurin. J. Biol. Chem. *280*, 12683–12689.

Wen, Z., Guirland, C., Ming, G.L., and Zheng, J.Q. (2004). A CaMKII/calcineurin switch controls the direction of Ca(2+)-dependent growth cone guidance. Neuron *43*, 835–846.

Willis, D., Li, K.W., Zheng, J.Q., Chang, J.H., Smit, A., Kelly, T., Merianda, T.T., Sylvester, J., van Minnen, J., and Twiss, J.L. (2005). Differential transport and local translation of cytoskeletal, injury-response, and neurodegeneration protein mRNAs in axons. J. Neurosci. *25*, 778–791.

Wills, Z., Emerson, M., Rusch, J., Bikoff, J., Baum, B., Perrimon, N., and Van Vactor, D. (2002). A Drosophila homolog of cyclase-associated proteins collaborates with the Abl tyrosine kinase to control midline axon pathfinding. Neuron *36*, 611–622.

Wong, K., Ren, X.R., Huang, Y.Z., Xie, Y., Liu, G., Saito, H., Tang, H., Wen, L., Brady-Kalnay, S.M., Mei, L., et al. (2001). Signal transduction in neuronal migration: roles of GTPase activating proteins and the small GTPase Cdc42 in the Slit-Robo pathway. Cell *107*, 209–221.

Wong, E.V., Kerner, J.A., and Jay, D.G. (2004). Convergent and divergent signaling mechanisms of growth cone collapse by ephrinA5 and slit2. J. Neurobiol. *59*, 66–81.

Wu, K.Y., Hengst, U., Cox, L.J., Macosko, E.Z., Jeromin, A., Urquhart, E.R., and Jaffrey, S.R. (2005). Local translation of RhoA regulates growth cone collapse. Nature *436*, 1020–1024.

Zakharenko, S., and Popov, S. (2000). Plasma membrane recycling and flow in growing neurites. Neuroscience *97*, 185–194.

Zhang, X., and Poo, M.M. (2002). Localized synaptic potentiation by BDNF requires local protein synthesis in the developing axon. Neuron *36*, 675–688.

Zhang, H.L., Eom, T., Oleynikov, Y., Shenoy, S.M., Liebelt, D.A., Dictenberg, J.B., Singer, R.H., and Bassell, G.J. (2001). Neurotrophin-induced transport of a beta-actin mRNP complex increases beta-actin levels and stimulates growth cone motility. Neuron *31*, 261–275.

Zheng, J.Q., Kelly, T.K., Chang, B., Ryazantsev, S., Rajasekaran, A.K., Martin, K.C., and Twiss, J.L. (2001). A functional role for intra-axonal protein synthesis during axonal regeneration from adult sensory neurons. J. Neurosci. *21*, 9291–9303.

Zhou, Q., Homma, K.J., and Poo, M.M. (2004). Shrinkage of dendritic spines associated with long-term depression of hippocampal synapses. Neuron *44*, 749–757.

Zimmer, M., Palmer, A., Kohler, J., and Klein, R. (2003). EphB-ephrinB bi-directional endocytosis terminates adhesion allowing contact mediated repulsion. Nat. Cell Biol. *5*, 869–878.